Exploring Reaction Mechanism for Ammonia/Methane Combustion via Reactive Molecular Dynamics Simulations

Jing Wang[a], Xi Zhuo Jiang[a*], Kai H. Luo[b*]

[a] *School of Mechanical Engineering and Automation, Northeastern University, Shenyang, 110819, China*

[b] *Department of Mechanical Engineering, University College London, Torrington Place, London WC1E 7JE, United Kingdom*

*Corresponding author.

jiangxz@mail.neu.edu.cn(XZJ); k.luo@ucl.ac.uk (KHL)

Abstract

Ammonia has gained growing attention as a carbon-free fuel. However, extensive studies are still needed to clarify and complete reaction mechanisms for ammonia combustion over a wide range of conditions. In the present study, a series of reactive molecular dynamics simulations that could reproduce the ammonia/methane (NH_3/CH_4) combustion in air at high temperature and pressure conditions were conducted. Results show that high temperature accelerates the consumption of NH_3 and affects the yield of nitrogen oxides (NOx). Meanwhile, high pressure accelerates the NH_3 consumption, which could be partly attributed to the frequent energetic collisions, and influences the formation of NOx. To understand the mechanism for NOx formation, the reaction pathways of NH_3/CH_4 combustion at high pressures were generated by tracing the trajectories of reacting atoms. Results suggest that high pressure complicates reaction pathways of NH_3/CH_4 combustion as it enhances the molecular/atomic collisions. By comparing with five popular NH_3/CH_4 combustion mechanisms, new intermediates and elementary reactions revealed by this study are identified. The activation energies for a few featured elementary reactions are calculated as well. The activation energies obtained from the present study agree with previous results from combustion kinetics studies. The present study demonstrates the feasibility to generate reaction network via tracing the atomic events in a reacting system and that the reactive molecular dynamics is a cost-effective tool in revealing in-depth reaction mechanisms under extreme conditions.

Keywords: ammonia/methane; combustion; reaction mechanism; nitrogen oxides (NOx); reactive molecular dynamics

1. Introduction

Ammonia (NH_3) has been identified as an important means to support a transition to hydrogen economy and has gained growing attention from all over the world as one of the best hydrogen carriers. Ammonia can be used directly as a carbon-free fuel for a wide range of end-use modalities [1], such as vehicle engines [2], marine engines [3], and combustion engines for power generators [4]. However, the high auto-ignition temperature and the low flame speed of ammonia [5, 6] often lead to incomplete combustion and thereby poor engine performance. By adding active gases/fuels [7, 8], like methane (CH_4), to the combustion system, the overall combustion performance could be significantly improved [9].

Recent studies have investigated the flame properties [10, 11], ignition [12], blow-off and transient characteristics [13] and pollutant emissions [14] of NH_3/CH_4 combustion. Meanwhile, worldwide efforts have been made to reveal the ammonia combustion kinetics [15-21]. A popular way to construct combustion kinetics is to identify the intermediates of combustion via experimental detection and then to form reaction mechanisms based on kinetic theories; some reaction networks can also be generated by extracting relevant reactions from automated reaction database which comprises various types of chemical reaction templates [22]. Such methods have had considerable successes but are very costly and time-consuming, since it is very difficult to capture all the intermediates via experiments during the combustion process. Experimental and/or theoretical uncertainties have also led to very different reaction mechanics of ammonia and its fuel blends. Currently, wide disparities exist in the prediction of ammonia combustion characteristics by different existing kinetic mechanisms. For example, a comparative study [23] suggests that the flame speeds predicted by Nakamura's [24] and Stagni's [25] mechanisms are quite close, whereas the predominant reactions in individual mechanisms are different. In light of this, further studies, especially with novel methodologies, are needed for developing NH_3/CH_4 reaction mechanisms that are valid over a wide range of conditions.

At the microscale, chemical reactions occur when molecules/atoms come close, with proper relative orientations, energies and angular momentum, to form new chemical bonds and to break existing ones. Thus, the reaction network can be deduced if the trajectories of atoms involved in a combustion system are known. Molecular dynamics (MD) is a computational method, governed by Newton's Law of Motion, which can mimic the molecular/atomic behaviour at the atomic scale. By incorporating appropriate force fields (a set of parameters to calculate the molecular/atomic interactions), MD is able to reproduce the atomic trajectories when a chemical reaction occurs. MD, therefore, provides an alternative way to generate reaction mechanisms by interrogating the atomic events in a reaction.

The aim of this study is to reveal the reaction pathways for NH_3/CH_4 combustion in air, especially at high temperature (T) and high pressure (p) conditions, based on atomistic simulations. A series of MD simulations with a set of reactive force field (ReaxFF) parameters are conducted to imitate the NH_3/CH_4 combustion in air. Reaction pathways for the combustion process are then generated by tracing the motions of all the intermediate species. A special attention is paid to the formation of nitrogen oxides (NOx) as the main pollutant from the NH_3/CH_4 combustion. Reaction pathways found from this study are also compared with those from the kinetics-based methods.

2. Methods

2.1 Reactive force field molecular dynamics (ReaxFF MD)

ReaxFF MD is a novel type of MD techniques that uses the concept of bond order to model the interactions within a chemical system. By making each atomic interaction bond order dependent, MD can provide a dynamic description of each atomic and molecular interaction that does not depend on the predefined reactive sites. The implementation of bond order dependent feature is done by a detailed parameterization of the atomic, bonding, angle, and torsion properties of each particle and interaction within the system, against quantum and experimental data [26]. The forces on each atom are derived from the energy expression given as follows:

$$E_{\text{system}} = E_{\text{bond}} + E_{\text{over}} + E_{\text{under}} + E_{\text{lp}} + E_{\text{val}} + E_{\text{tor}} + E_{\text{vdW}} + E_{\text{Comb}} \quad (1)$$

where E_{system} is the total energy, and the first six terms contributing to the bonded energy on the right-hand side of Eq. (1) are the bond, over-coordination penalty, under-coordination, lone-pair, valence angle and torsion energies, respectively. The last two terms on the right-hand side contributing to the non-bonded terms are the van der Waals and electrostatic energies, respectively. Details about the history and development about the ReaxFF MD can be found in Ref. [27]. By combining quantum chemistry's capability for chemical reactions and classic MD's computational efficiency, ReaxFF MD has found applications in diverse fields including catalytic reactions [28, 29], field-assisted combustion [30, 31] and soot formation [32].

2.2 Case set-ups

The focus of this study is NH_3/CH_4 combustion in air at high temperature and high pressure conditions. In the present MD simulations, the number of molecules for NH_3, CH_4, O_2 and N_2 are 20, 10, 200 and 780, respectively. Here, more O_2 and N_2 molecules than the equivalence ratio were included to ensure the complete reaction of the fuel. Different temperatures and pressures were set for each case, as listed in Table 1. Cases 1 to 7 were designed to investigate the temperature effects on reactions with a constant density of the system. Cases 8 to 12 focused on the impact of pressure on combustion. Five replicates with different initial configurations were simulated for individual cases. 60 simulations were conducted in total.

Table 1 Case setups in the present study.

case	*T*, K	*p*, atm	Side length, Å
1	2400	41.3	200
2	2600	44.7	200
3	2800	48.2	200
4	3000	51.6	200
5	3200	55.1	200
6	3400	58.5	200
7	3600	61.9	200
8	2800	24.1	251.98
9	2800	96.4	158.74
10	2800	193	125.99
11	2800	385	100
12	2800	482	92.83

2.3 Computational details and post-processing

In the model construction, NH_3, CH_4, O_2 and N_2 molecules were randomly placed in a cubic simulation domain (Fig. 1) with the aid of PACKMOL [33] codes. The side length of the cubic domain varies among different cases, as listed in Table 1. Before "production" simulations, equilibrium simulations were conducted to reach energy minimization at 300 K for 40 ps. The system was then gradually heated from 300 K to the designated temperature in a period of 500 ps. Afterwards, the temperature was kept constant and the production simulations were finished until NH_3 was completely consumed.

ReaxFF parameters for systems containing C/N/H/O [34, 35] elements were selected to calculate the atomic interactions (the force field file parameters is provided in the Supplementary Data 1). A canonical (NVT) ensemble under the Nosé–Hoover thermostat algorithm with a damping constant of 100 fs was used to maintain temperature. The atomic trajectories were updated with a time step of 0.1 fs and recorded every 1 ps. All the simulations were implemented with the USER-REAXC package in the LAMMPS platform [36].

In the post-processing, a bond order cutoff of 0.3 [30] was selected for molecular recognition in identifying intermediates and products formed during the MD simulations. Data were averaged over the five replicates, and reaction pathways were generated based on all the five replicates. All the post-processing was implemented using our in-house scripts. The reaction pathways were summarised with the latest version of the ChemTraYzer scripts [37] and our in-house codes. The visualization of molecular structures was performed by the VMD package [38]. Unless otherwise indicated, data with error bars represent mean ± SD (standard deviations).

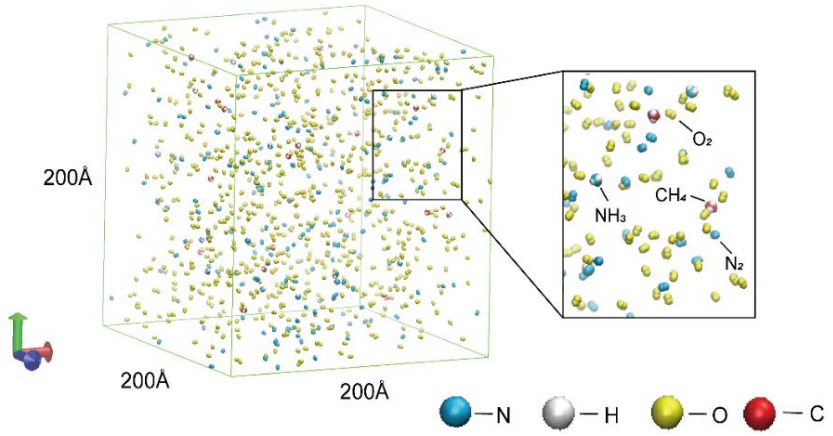

Figure 1 Initial configuration of a typical simulation. Gas molecules are randomly placed in a cubic box. (For clarity, O_2 and N_2 are partly shown.)

2.4 Validation of the ReaxFF MD method

The reliability and effectiveness of the ReaxFF MD method have been validated via a wide range of applications, as reviewed in [27], including fuels or processes comprising C/H/O/N elements, such as RDX ($C_3H_6N_6O_6$) [39], TATB($C_3H_6N_6O_6$) [34] and decomposition of hydrazine (N_2H_4) in hydrogen peroxide (H_2O_2) [35].

3. Results and Discussion

3.1 Effects of temperature and pressure on NH_3/CH_4 combustion

The effects of temperature on NH_3/CH_4 combustion in air were investigated in terms of the consumption of NH_3, activation energy, and the yield of NOx (NO and NO_2), as shown in Figures 2a-2c. (Time evolutions of NO and NO_2 at different temperatures are shown in Fig. S1) As expected, the temperature accelerates the consumption of NH_3. The decomposition of NH_3 as shown in Fig. 2a follows almost a linear pattern. Thus, a zeroth order reaction can be used to calculate the rate constant (k) for NH_3 decomposition, i.e., $d[NH_3]/dt=k$. The activation energy (Ea) for NH_3 decomposition was calculated by the slope of the $\ln k - 1/T$ curve (Fig. 2b) *as per* Arrhenius equation. The Ea for ammonia decomposition obtained from this study is 95.89 kJ/mol and is lower than the activation energy of pure ammonia combustion reported in previous studies (NH_3 combustion in O_2/Ar, Ea = 165.3 kJ/mol, p = 11 atm) [40] and our MD simulations (NH_3 combustion in N_2/O_2, Ea = 108.25 kJ/mol, p = 48.2 atm).

The lower activation energy demonstrates that the addition of CH_4 enhances the combustion of NH_3. The numbers of NO and NO_2 molecules were counted at the instant of 15000 ps in the production simulations. As shown in Fig. 2c, when the temperature is below 3000 K, the formation of NOx follows the thermal mechanism and increases with temperature; when the temperature is over 3000 K, decrease in the yield of NOx is observed at 3200 K and 3600 K. Scrutiny of the elementary reactions suggests that the number NOx-producing reactions is reduced at 3200 K whilst the number of NOx-consuming reactions increases at 3600 K.

The effects of pressure on NH_3/CH_4 combustion in air were explored in terms of the consumption of NH_3, intermolecular collision frequencies, and the yield of NOx, as shown in Figures 2d-2f, respectively. (Time evolutions of NO and NO_2 at different pressures are shown in Fig. S2.) In Fig. 2d, high pressure significantly increases the reaction rate of NH_3/CH_4 combustion by promoting the conversion of NH_3. To find out the mechanism for the promoting effects of pressure on reaction rate, the collision frequencies within NH_3 molecules and between NH_3 and CH_4 molecules at the very beginning of the production reactions were calculated at varying pressures. At high pressures, molecules are packed closely, and the possibility that two molecules encounter increases, resulting in an increase in collision frequency, as suggested in Fig. 2e. It is reasonable to assume that the probability distributions (a Boltzmann-like distribution) of energy for effective collisions are the same among all the pressure cases (cases 7-12), as all the cases share the same temperature. Thus, as suggested by the collision theory, the fast consumption of NH_3 at high pressures can be partly attributed to the high collision frequencies among molecules. The numbers of NOx at the end of reactions were compared at different pressures. In Fig. 2f, a non-linear trend of NOx generation with the rise of pressure was observed: the number of NOx increases with pressure until a peak is reached at p = 193 atm; afterwards, high pressure inhibits the generation of NOx.

According to Fig. 2, both high temperature and high pressure can accelerate the consumption of ammonia. In cases 1 to 7, the volume (density) is kept constant, which is a more common scenario in practice. The temperature increases from 2400 K to 3600 K in cases 1 to 7 could induce pressure increase which contributes to the fast consumption of NH_3 at high temperature conditions. The effects

of pressure and temperature on the acceleration of ammonia combustion rates were quantified, and results suggest that temperature has more significant effects on changing the reaction rate its pressure counterpart. (Details can be found in Supplementary File.)

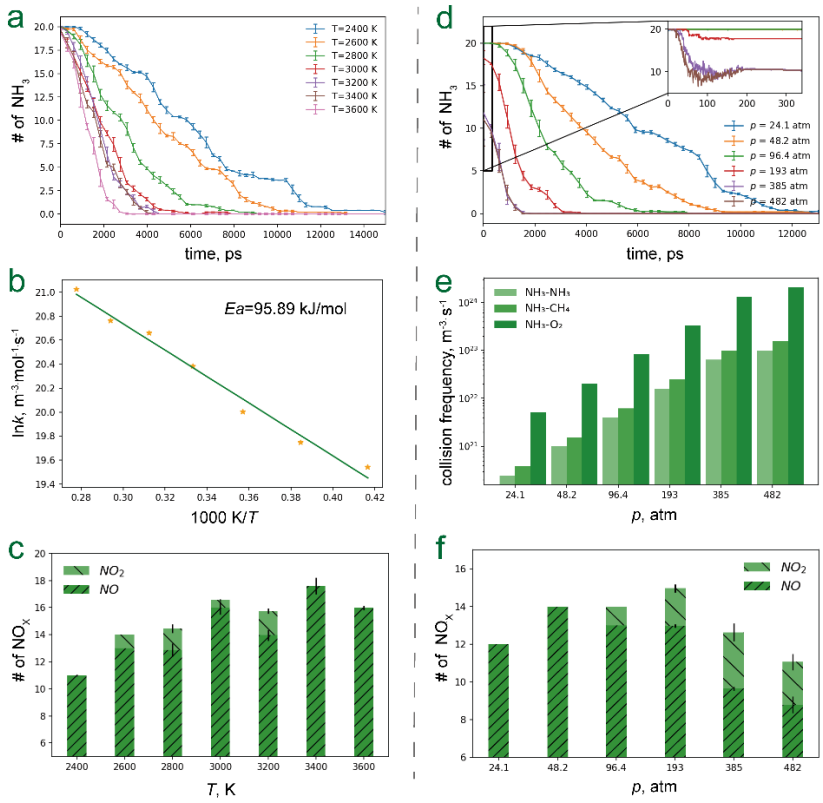

Figure 2 Effects of temperature and pressure on NH_3/CH_4 combustion. a. Consumption of NH_3 at different temperatures (Data were time-averaged every 300 ps.); b. Activation energy for ammonia reaction derived from this study; c. NOx formation at varying temperatures; d. Consumption of NH_3 at different pressures (Data were time-averaged every 300 ps.); e. Collision frequencies at different pressures; f. NOx formation under varying pressures.

3.2 Reaction pathways

To examine whether a high pressure could increase the complexity of the reactions as it increases the collision frequencies, the reaction mechanisms for NH_3/CH_4 combustion in air under varying pressure conditions were generated and discussed here.

The number of species (including reactants and intermediates) and number of elementary reactions at varying pressures were compared in Fig. 3 (Details about the species and reactions at different

pressures are provided in the Supplementary Data 2-7.). The number of elementary reactions rises with pressure, suggesting that the pressure complicates the NH_3/CH_4 combustion. At 48.2 atm, a local peak in the number of species is observed. Scrutiny of the species shows that intermediates with two carbon atoms (C_2) are produced at 48.2 atm but these C_2 species only exist for a short time and are consumed quickly after generation. Figure 3 also shows the number of reactions which lead to the formation of NOx. A higher pressure induces more NOx formation reactions.

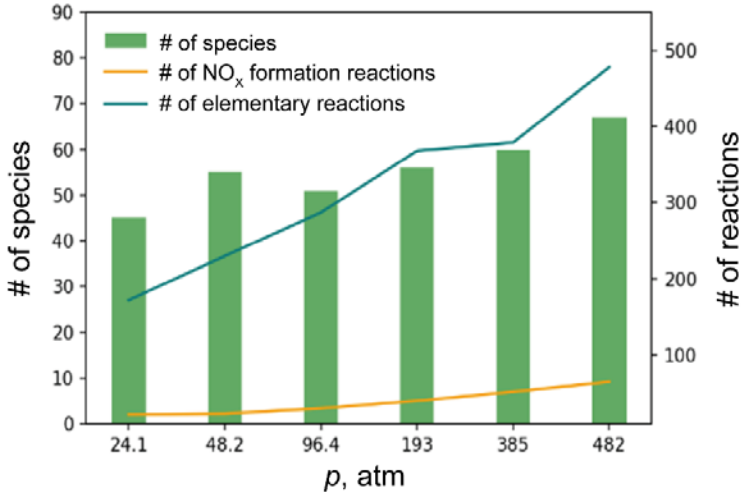

Figure 3 Numbers of species and reactions at varying pressures.

In Table 2, the numbers of species and the elementary reactions at p = 48.2 atm were compared with five popular NH_3/CH_4 combustion mechanisms, e.g., GRI Mech 3.0 [15], Okafor [16], Tian [19] and San Diego [17] and Glarborg [18] . The digits in round brackets represent the numbers of N-containing species and elementary reactions. In the San Diego mechanism, the original mechanism and the nitrogen chemistry are provided separately in the original website. In Table 2, these two mechanisms are combined.

To understand the formation mechanism of NOx, the reaction network for key N-containing intermediates were extracted in Fig. 4. The p = 48.2 atm case was used to generate the reaction network. The reactions of NOx formation were also mapped in the five popular NH_3/CH_4 mechanisms, and common reactions were labelled in square brackets. The comparison indicates that MD simulations are able to discover new reactions of decomposition (+M), reactions with H, H_2, HO_2, O, O_2, NH and NO

and reactions with intermediates uniquely discovered in this study, like O_3. Lists of new species discovered by the present study can be found in Supplementary Data 8.

Table 2 Reaction mechanisms for NH_3/CH_4 combustion. Digits in brackets are for those containing N atoms.

Name	# of species/# of reactions	Ref.
GRI MECH 3.0	53 (18) / 325 (108)	[15]
Okafor *et al.*	59 (24) / 356 (139)	[16]
Tian *et al.*	84 (40) / 703 (400)	[19]
San Diego*	70 (11) / 309 (29)	[17]
Glarborg *et al.*	151 (83) / 1395 (866)	[18]
This work	55 (24) / 230 (118)	/

*The complete San Diego mechanism (excl. nitrogen) and the nitrogen chemistry are combined here.

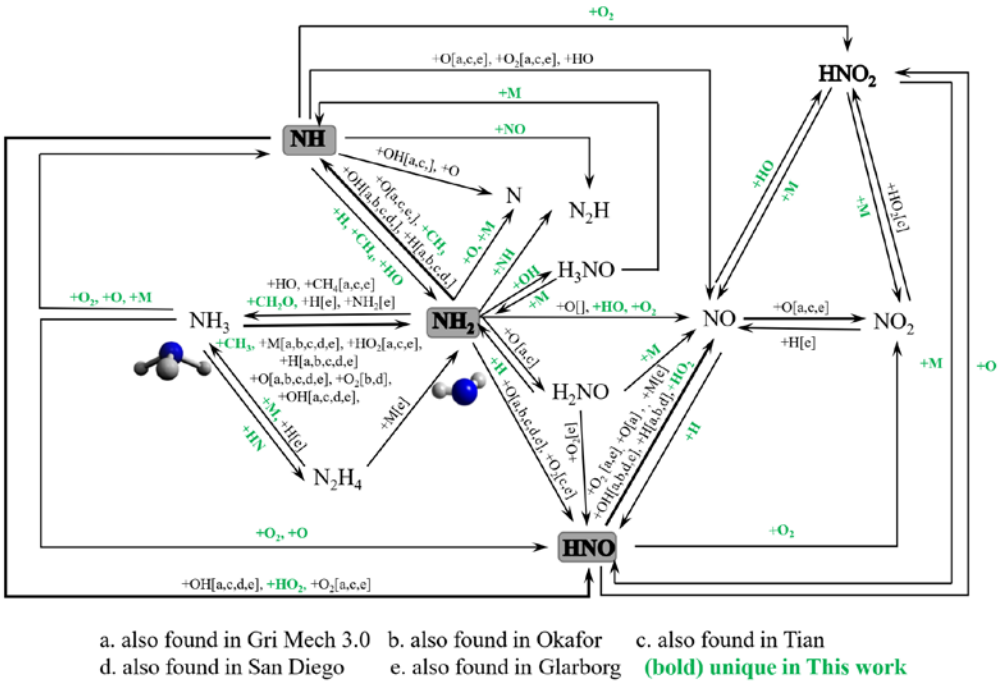

Figure 4 NOx formation in NH_3/CH_4 combustion based on ReaxFF MD simulations. Elementary reactions reported in five popular mechanisms are labelled in square brackets. The pathways via which most of reactants are converted to products are labelled by bold lines. NH, NH_2 and N_2H will form N_2. For clarity, the reactions to form N_2 are not listed.

Herein, five sets of NH_3/CH_4 combustion mechanisms were compared in Fig. 4. For the mechanisms of GRI MECH 3.0, Okafor, San Diego and Glarborg, radicals containing C atom attend in N chemistry at a quite late stage when NH_3 is converted to N, N_2 and NO. By contrast, Tian and the present mechanisms suggest that radicals with C atom could participate in N chemistry at the early stage of NH_3 decomposition. For example, both Tian and the present mechanisms reveal that CH_4 could react with NH_2, and the present mechanism further indicates that the collisions between CH_3 and NH_3 could cause the decomposition of NH_3 to NH_2. In the present study, over 90% of elementary reactions where NH_3 molecules are directly converted NH_2 require the participation of OH, O and H radicals; CH_3 accounts for 3% direction conversion from NH_3 to NH_2.

The present mechanism also reveals NH as an active radical in N chemistry. The formation of N_2 is also found in our ReaxFF MD simulations, and all reactions leading to N_2 formation are provided in Fig. 5. NH, NH_2 and N_2H in Fig.4 are all active radicals for N_2 formation.

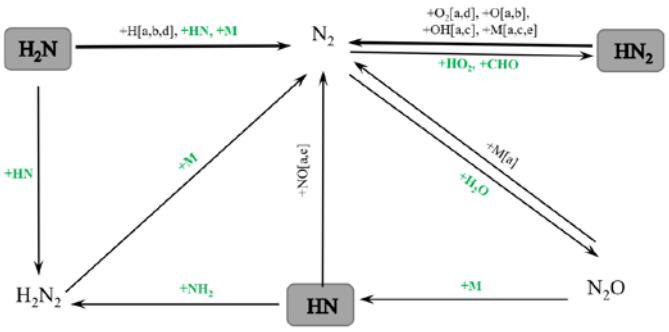

a. also found in Gri Mech 3.0 b. also found in Okafor c. also found in Tian
d. also found in San Diego e. also found in Glarborg **(bold) unique in This work**

Figure 5 Reaction pathways for N_2 generation obtained from the present study.

3.3 Activation energy of NH_3 hydrogen-loss reactions

In Fig. 4, seven pathways via which NH_3 is converted to NH_2, are identified. The bimolecular reactions of NH_3 with CH_3 and O_2 are newly reported in the present study. To better understand the new reactions, the activation energy for NH_3+O_2 was calculated based on cases 1 to 7. (The occurrence of NH_3 + CH_3 is less frequent, and the data obtained from this study is not sufficient to support a reliable

result for activation energy. Here, only the activation energy for NH_3+O_2 is provided.) For reference, the activation energies for two unimolecular hydrogen-loss reactions of ammonia (i.e., $NH_3 \rightarrow NH_2+H$ and $NH_3 \rightarrow NH+H_2$) were also calculated. As shown in Fig. 6, the activation energy of $NH_3+O_2 \rightarrow NH_2+HO_2$ is in between those of $NH_3 \rightarrow NH_2+H$ and $NH_3 \rightarrow NH+H_2$.

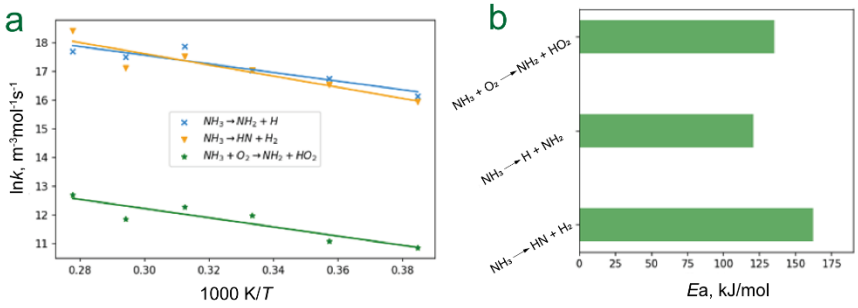

Figure 6 Activation energies for three NH_3 hydrogen-abstraction reactions. a. ln$k$-T curves of Arrhenius Equation for three NH_3 hydrogen-abstraction reactions. b. Activation energy obtained from the slopes of the ln$k$-T curves in a.

The other four hydrogen-abstraction reactions of NH_3 were also reported in previous studies. The activation energies for the four reactions were then calculated and compared in Table 3. Generally, the activation energy obtained from the present MD study agrees well with previous studies, especially in terms of order of magnitude, which demonstrates that the ReaxFF MD could provide satisfactory results for reaction kinetics. The results for Ea can be further improved via quantum mechanism calculations.

Table 3 Comparisons of Ea for four shared reactions.

Reactions	Previous studies	This work
$NH_3+H \rightarrow NH_2+H_2$	9915[15]	9896
$NH_3+O \rightarrow NH_2+OH$*	6465[17]	6473
$NH_3+OH \rightarrow NH_2+H_2O$**	955[15]	716
$NH_3+HO_2 \rightarrow NH_2+H_2O_2$	22000[19]	24684

* The reaction rate is calculated by $k=AT^m\exp(-Ea/RT)$. m is 1.9 in Ref. [17] and 1 in this study.

** The reaction rate is calculated by $k=AT^m\exp(-Ea/RT)$. m is 1.6 in Ref. [15] and 1 in this study.

3.4 Discussion

The present study features the reaction pathways for NH_3/CH_4 combustion at high pressures, as mechanisms for high-pressure combustion are lacking due to difficulty and high cost of conducting experiments under such conditions. For the five mechanisms mentioned in Table 2, Tian and Okafor mechanisms were originally developed based on data from combustions at low pressures; according to the official websites, GRI MECH 3.0 and San Diego mechanisms have been occasionally performed to combustion at high pressure conditions. For NH_3/CH_4 combustion at high pressures, radicals (like NH, O_2 and HO_2) are more active and energetic than at low pressures, inducing additional N-containing species reaction pathways as highlighted in Fig. 4. The high pressure also promotes the decomposition of radicals (e.g., HNO, N_2H_4, H_3NO_2, HNO_2, etc) as energetic collisions are more likely to happen as demonstrated in Fig. 2e.

The generation of NOx can be categorized into three types: thermal NOx (NOx is formed from N_2 in the air), fuel NOx (NOx is formed from N-containing fuel) and prompt NOx (NOx is formed by atmospheric nitrogen with hydrocarbon radicals). In the present study, fuel NOx is predominant following the chain reactions in Fig. 4. It is not straightforward to identify the thermal NOx in this study, as NH_3 could convert to N_2 via NH_2, NH and N_2H as shown in Fig. 4 and Fig. 5. In addition, the reactions of N_2 and hydrocarbon were occasionally spotted in the present study, e.g., $N_2+CH_2 \rightarrow CH_2N_2$ at 96.4 atm (Supplementary Data 4) and $N_2+CH_3+O \rightarrow CH_2O+HN_2$ at 385 atm (Supplementary Data 6); however, these reactions will not directly lead to the formation of NOx, and prompt NOx was scarcely spotted.

In this study, a series of reaction pathways and reaction rates for NH_3/CH_4 combustion in air at various high pressure conditions were proposed. Activation energies for a few reactions were solved as well. To form a complete set of reaction mechanisms that can be used to simulate flame behaviour, calculation of activation energy for every individual elementary reaction is required, which would require additional efforts. Activation energies can be also obtained via systematic quantum chemistry calculations. Alternatively, machine learning could offer rapid and accurate prediction of activation energies of elementary reactions [41, 42].

4. Conclusions

In this study, a series of ReaxFF MD simulations were conducted to simulate the NH_3/CH_4 combustion in air at various temperatures and pressures. High temperature accelerates the consumption of NH_3, which agrees with experimental observation. The activation energy for the NH_3 combustion in the presence of CH_4 was calculated as well, and the result suggests that the addition of CH_4 improves the combustion performance. Meanwhile, high pressures promote the conversion of NH_3 by augmenting the collision frequency of reacting atoms. In addition, the influence of high pressure on the yield of NOx is non-linear. To understand the mechanism for NOx formation, the reaction pathways of NH_3/CH_4 combustion at high pressures were constructed by tracing the trajectories of reacting atoms. Results suggest that high pressure complicates reaction pathways of NH_3/CH_4 combustion as it enhances the molecular/atomic collisions. By comparing with five popular NH_3/CH_4 combustion mechanisms, new intermediates and elementary reactions are identified in this study. Furthermore, the activation energies for a few featured elementary reactions were calculated. The activation energies obtained from the present study agree with previous results from combustion kinetics studies. The present study demonstrates the feasibility to generate reaction network via tracing the atomic events in a reacting system. The ReaxFF MD is a valuable tool in revealing in-depth reaction mechanisms, which complements experimental and kinetics-based studies. In future work, activation energies for individual elementary reactions will be calculated to form a complete set of reaction mechanisms for NH_3/CH_4 combustion and to facilitate the prediction of the combustion behaviour.

Acknowledgements

This work is supported by National Natural Science Foundation of China (Grant No. 52106132).

Supplementary materials

Supplementary File: Figure S1, S2 and effects of pressure and temperature on NH_3 consumption rates; Supplementary Data 1: reactive force field parameters; Supplementary Data 2-7: species and

reaction pathways at p = 24.1 atm, 48.2 atm, 96.4 atm, 193 atm, 385 atm and 482 atm, respectively; Supplementary Data 8: common and unique species reported in the present study.

References

[1] D.R. MacFarlane, P.V. Cherepanov, J. Choi, B.H.R. Suryanto, R.Y. Hodgetts, J.M. Bakker, F.M. Ferrero Vallana, A.N. Simonov. A roadmap to the ammonia economy. Joule 2020;4:1186-1205. https://doi.org/10.1016/j.joule.2020.04.004

[2] P. Dimitriou, R. Javaid. A review of ammonia as a compression ignition engine fuel. Int J Hydrog Energy 2020;45:7098-7118. https://doi.org/10.1016/j.ijhydene.2019.12.209

[3] A. Valera-Medina, F. Amer-Hatem, A.K. Azad, I.C. Dedoussi, M. de Joannon, R.X. Fernandes, P. Glarborg, H. Hashemi, X. He, S. Mashruk, J. McGowan, C. Mounaim-Rouselle, A. Ortiz-Prado, A. Ortiz-Valera, I. Rossetti, B. Shu, M. Yehia, H. Xiao, M. Costa. Review on Ammonia as a Potential Fuel: From Synthesis to Economics. Energy Fuels 2021;35:6964-7029. https://doi.org/10.1021/acs.energyfuels.0c03685

[4] A. Sánchez, E. Castellano, M. Martín, P. Vega. Evaluating ammonia as green fuel for power generation: A thermo-chemical perspective. Appl Energy 2021;293. https://doi.org/10.1016/j.apenergy.2021.116956

[5] W.S. Chai, Y. Bao, P. Jin, G. Tang, L. Zhou. A review on ammonia, ammonia-hydrogen and ammonia-methane fuels. Renew Sust Energ Rev. 2021;147. https://doi.org/10.1016/j.rser.2021.111254

[6] R. Zhang, L. Chen, H.Wei, J. Li, R. Chen, J. Pana. Understanding the difference in combustion and flame propagation characteristics between ammonia and methane using an optical SI engine. Fuel 2022;324:124794. https://doi.org/10.1016/j.fuel.2022.124794

[7] H. Kobayashi, A. Hayakawa, K.D.Kunkuma A. Somarathne, Ekenechukwu C. Okafor. Science and technology of ammonia combustion. Proc Combust Inst 2019;37:109-133. https://doi.org/10.1016/j.proci.2018.09.029

329 [8] S. Wüthrich, P. Cartier, Pascal Süess, B. Schneider, P. Obrecht, K. Herrmann. Optical investigation
330 and thermodynamic analysis of premixed ammonia dual-fuel combustion initiated by dodecane pilot
331 fuel. Fuel 2022;12:100074. https://doi.org/10.1016/j.jfueco.2022.100074
332 [9] H. Xiao, S. Lai, A. Valera-Medina, J. Li, J. Liu, H. Fu. Study on counterflow premixed flames using
333 high concentration ammonia mixed with methane. Fuel 2020;275:117902.
334 https://doi.org/10.1016/j.fuel.2020.117902
335 [10] H. Xiao, A. Valera-Medina, P.J. Bowen. Study on premixed combustion characteristics of co-
336 firing ammonia/methane fuels. Energy 2017;140:125-135.
337 https://doi.org/10.1016/j.energy.2017.08.077
338 [11] T. Shu, Y. Xue, Z. Zhou, Z. Ren. An experimental study of laminar ammonia/methane/air
339 premixed flames using expanding spherical flames. Fuel 2021;290:120003.
340 https://doi.org/10.1016/j.fuel.2020.120003
341 [12] B. Shu, X. He, C.F. Ramos, R.X. Fernandes, M. Costa. Experimental and modeling study on the
342 auto-ignition properties of ammonia/methane mixtures at elevated pressures. Proc Combust Inst
343 2021;38:261-268. https://doi.org/10.1016/j.proci.2020.06.291
344 [13] M. Zhang, X. Wei, J. Wang, Z. Huang, H. Tan. The blow-off and transient characteristics of co-
345 firing ammonia/methane fuels in a swirl combustor. Proc Combust Inst 2021;38:5181-5190.
346 https://doi.org/10.1016/j.proci.2020.08.056
347 [14] G.B. Ariemma, G. Sorrentino, R.Ragucci, M. de Joannonb, P. Sabiab. Ammonia/Methane
348 combustion: Stability and NOx emissions. Combust Flame 2022;241:112071.
349 https://doi.org/10.1016/j.combustflame.2022.112071
350 [15] Gregory P. Smith, David M. Golden, Michael Frenklach, Nigel W. Moriarty, Boris Eiteneer,
351 Mikhail Goldenberg, C. Thomas Bowman, Ronald K. Hanson, Soonho Song, J. William C. Gardiner,
352 Vitali V. Lissianski, Z. Qin. GRI Mech 3.0. http://www.me.berkeley.edu/gri_mech/.
353 [16] E.C. Okafor, Y. Naito, S. Colson, A. Ichikawa, T. Kudo, A. Hayakawa, H. Kobayashi.
354 Experimental and numerical study of the laminar burning velocity of CH_4–NH_3–air premixed flames.
355 Combust Flame 2018;187:185-198. https://doi.org/10.1016/j.combustflame.2017.09.002

[17] Mechanical and Aerospace Engineering (Combustion Research), Chemical-kinetic mechanisms for combustion applications. mechanical and aerospace engineering http://web.eng.ucsd.edu/mae/groups/combustion/mechanism.html.

[18] P. Glarborg, J.A. Miller, B. Ruscic, S.J. Klippenstein. Modeling nitrogen chemistry in combustion. Prog Energy Combust Sci 2018;67:31-68. https://doi.org/10.1016/j.pecs.2018.01.002

[19] Z. Tian, Y. Li, L. Zhang, P. Glarborg, F. Qi. An experimental and kinetic modeling study of premixed $NH_3/CH_4/O_2$/Ar flames at low pressure. Combust Flame 2009;156:1413-1426. https://doi.org/10.1016/j.combustflame.2009.03.005

[20] A.M. Elbaz, S. Wang, T. Guiberti, W.L. Roberts. Review on the recent advances on ammonia combustion from the fundamentals to the applications. Fuel Commun 2022;10:100053. https://doi.org/10.1016/j.jfueco.2022.100053

[21] H. Mikulčić, J. Baleta, X. Wang, J. Wang, F. Qi, F. Wang. Numerical simulation of ammonia/methane/air combustion using reduced chemical kinetics models. Fuel 2021;46:23548-23563. https://doi.org/10.1016/j.ijhydene.2021.01.109

[22] P.P. Plehiers, G.B. Marin, C.V. Stevens, K.M. Van Geem. Automated reaction database and reaction network analysis: extraction of reaction templates using cheminformatics. J Cheminform 2018;10:11. https://doi.org/10.1186/s13321-018-0269-8

[23] A. Karan, G. Dayma, C. Chauveau, F. Halter. Experimental study and numerical validation of oxy-ammonia combustion at elevated temperatures and pressures. Combust Flame 2022;236:111819. https://doi.org/10.1016/j.combustflame.2021.111819

[24] H. Nakamura, S. Hasegawa. Combustion and ignition characteristics of ammonia/air mixtures in a micro flow reactor with a controlled temperature profile. Proc Combust Inst 2017;36:4217-4226. https://doi.org/10.1016/j.proci.2016.06.153

[25] A. Stagni, C. Cavallotti, S. Arunthanayothin, Y. Song, O. Herbinet, F. Battin-Leclerc, T. Faravelli. An experimental, theoretical and kinetic-modeling study of the gas-phase oxidation of ammonia. React Chem Eng 2020;5:696-711. https://doi.org/10.1039/c9re00429g

[26] M.F. Russo, A.C.T. van Duin. Atomistic-scale simulations of chemical reactions: bridging from quantum chemistry to engineering. Nucl Instrum Methods Phys Res B 2011;269:1549-1554. https://doi.org/10.1016/j.nimb.2010.12.053

[27] T.P. Senftle, S. Hong, M.M. Islam, S.B. Kylasa, Y. Zheng, Y.K. Shin, C. Junkermeier, R. Engel-Herbert, M.J. Janik, H.M. Aktulga, T. Verstraelen, A. Grama, A.C.T. van Duin. The ReaxFF reactive force-field: development, applications and future directions. NPJ Comput Mater, 2016;2:15011. https://doi.org/10.1038/npjcompumats.2015.11

[28] Y.R. Zhang, A.C.T. van Duin, K.H. Luo. Investigation of ethanol oxidation over aluminum nanoparticle using ReaxFF molecular dynamics simulation. Fuel 2018;234:94-100. https://doi.org/10.1016/j.fuel.2018.06.119

[29] Q. Chu, B. Shi, L. Liao, X. Zou, K.H. Luo, N. Wang. Reaction mechanism of the aluminum nanoparticle: physicochemical reaction and heat/mass transfer. J Phys Chem C 2020;124:3886-3894. https://doi.org/10.1021/acs.jpcc.9b11410

[30] X.Z. Jiang, M. Feng, W. Zeng, K.H. Luo. Study of mechanisms for electric field effects on ethanol oxidation via reactive force field molecular dynamics. Proc Combust Inst 2019;37:5525-5535. https://doi.org/10.1016/j.proci.2018.07.053

[31] X.Z. Jiang, K.H. Luo. Reactive and electron force field molecular dynamics simulations of electric field assisted ethanol oxidation reactions. Proc Combust Inst 2021;38:6605-6613. https://doi.org/10.1016/j.proci.2020.06.318

[32] C. Chen, X. Jiang. Molecular dynamics simulation of soot formation during diesel combustion with oxygenated fuel addition. Phys Chem Chem Phys 2020;22:20829-20836. https://doi.org/10.1039/d0cp01917h

[33] L. Martinez, R. Andrade, E.G. Birgin, J.M. Martinez. PACKMOL: a package for building initial configurations for molecular dynamics simulations. J Comput Chem 2009;30:2157-2164. https://doi.org/10.1002/jcc.21224

[34] L. Zhang, S.V. Zybin, A.C.T. van Duin, S. Dasgupta, W.A. Goddard, E.M. Kober. Carbon Cluster Formation during Thermal Decomposition of Octahydro-1,3,5,7-tetranitro-1,3,5,7-tetrazocine and

1,3,5-Triamino-2,4,6-trinitrobenzene High Explosives from ReaxFF Reactive Molecular Dynamics Simulations. J Phys Chem A 2009;113(40):10619–10640. https://doi.org/10.1021/jp901353a

[35] L. Zhang, A.C.T. van Duin, S.V. Zybin, W.A. Goddard. Thermal Decomposition of Hydrazines from Reactive Dynamics Using the ReaxFF Reactive Force Field. J Phys Chem B 2009;113(31):10770–10778. https://doi.org/10.1021/jp900194d

[36] A.P. Thompson, H.M. Aktulga, R. Berger, D.S. Bolintineanu, W.M. Brown, P.S. Crozier, A. Kohlmeyer, P.J. in 't Veld, S.G. Moore, T.D. Nguyen, R. Shan, M.J. Stevens, J. Tranchida, C. Trott, S.J. Plimpton, LAMMPS - a flexible simulation tool for particle-based materials modeling at the atomic, meso, and continuum scales. Comput Phys Commun 2022;271:108171. https://doi.org/10.1016/j.cpc.2021.108171

[37] M. Dontgen, M.D. Przybylski-Freund, L.C. Kroger, W.A. Kopp, A.E. Ismail, K. Leonhard. Automated discovery of reaction pathways, rate constants, and transition states using reactive molecular dynamics simulations. J Chem Theory Comput 2015;11:2517-2524. https://doi.org/10.1021/acs.jctc.5b00201

[38] W. Humphrey, A. Dalke, K. Schulten. VMD: Visual molecular dynamics. J Mol Graph 1996;14: 33-38. https://doi.org/10.1016/0263-7855(96)00018-5

[39] A. Strachan, E.M. Kober, A.C. van Duin, J. Oxgaard, W.A. Goddard. Thermal decomposition of RDX from reactive molecular dynamics. J Chem Phys 2005;122:54502. https://doi.org/10.1063/1.1831277

[40] O. Mathieu, E.L. Petersen. Experimental and modeling study on the high-temperature oxidation of ammonia and related NO_x chemistry. Combust Flame 2015;162:554-570. https://doi.org/10.1016/j.combustflame.2014.08.022

[41] K. Takahashi, I. Miyazato. Rapid estimation of activation energy in heterogeneous catalytic reactions via machine learning. J Comput Chem 2018;39:2405-2408. https://doi.org/10.1002/jcc.25567

[42] K. Jorner, T. Brinck, P.-O. Norrby, D. Buttar. Machine learning meets mechanistic modelling for accurate prediction of experimental activation energies. Chem Sci 2021;12:1163-1175. https://doi.org/10.1039/d0sc04896h